DEGREE PROJECT IN TECHNOLOGY,
SECOND CYCLE, 30 CREDITS
STOCKHOLM, SWEDEN 2023

First principles investigation of the thermal conductivity of Zr, ZrC, and ZrN

KTH Thesis Report

Daniel Karlsson

KTH ROYAL INSTITUTE OF TECHNOLOGY
SCHOOL OF ENGINEERING SCIENCES

TRITA-SCI-GRU 2023:351

Author

Daniel Karlsson, danielk5@kth.se
School of Engineering Sciences
KTH Royal Institute of Technology

Place for Project

Stockholm, Sweden

Examiner

Janne Wallenius
KTH Royal Institute of Technology

Supervisor

Pär Olsson
KTH Royal Institute of Technology

Abstract

The thermal conductivity and electrical resistivity of Zr, ZrC, and ZrN were calculated using first-principles density functional theory (DFT) and the Boltzmann transport equation. The electron-phonon scattering was modeled via the self-energy relaxation time approximation (SERTA), and the phonon-phonon scattering via the analogous single-mode relaxation time approximation (SMRTA).

The results obtained from Abinit's electron-phonon coupling code EPH is in good agreement with experimental reference data for Zr and ZrN. Notably, the calculated electrical resistivity of ZrC was found to be significantly lower than the available reference data, likely due to deviations from a perfect Zr/C stoichiometric ratio in the experimental samples. Additionally, it was observed that the calculated lattice thermal conductivity was overestimated at low temperatures, possibly attributed to the neglect of electron-phonon scattering that otherwise appears in metallic systems.

Keywords

Electron-phonon interaction, density functional theory, Boltzmann transport equation, first-principles, thermal conductivity, electrical resistivity, Abinit, Phono3py.

Sammanfattning

Värmeledningsförmågan och den elektriska resistiviteten för Zr, ZrC och ZrN beräknades med hjälp av täthetsfunktionalteori (DFT) och Boltzmanns transportekvation. Elektron-fononspridningen modellerades via *'self-energy relaxation time approximation'* (SERTA), och fonon-fononspridningen via den motsvarande *'single-mode relaxation time approximation'* (SMRTA).

Resultaten från Abinits elektron-fononkopplingskod EPH stämmer väl överens med experimentella referensdata för Zr och ZrN. Den beräknade elektriska resistiviteten för ZrC visade sig emellertid vara betydligt lägre än all tillgänglig referensdata, troligtvis på grund av avvikelser från ett perfekt Zr/C-stökiometriskt förhållande i de experimentella proverna. Dessutom observerades att det beräknade fononbidraget till värmeledningsförmågan överskattades vid låga temperaturer, vilket möjligen beror på försummelsen av elektron-fononspridning som annars framträder i metalliska system.

Nyckelord

Elektron-fononväxelverkan, täthetsfunktionalteori, Boltzmanns transportekvation, värmekonduktivitet, elektrisk resistivitet, Abinit, Phono3py.

Acknowledgments

Firstly, I am immensely grateful to my supervisor Pär Olsson, for his support, guidance, and encouragement through this project. He provided me with valuable insight and resources which was instrumental in shaping the quality of this research.

I would like to express my gratitude to my family for their unconditional love, encouragement, and unwavering belief in my abilities. Their constant support, understanding, and motivation have sustained me through the ups and downs of this challenging endeavor.

Simulations were performed with computing resources provided by KTH Parallelldatorcentrum (PDC) via the Fuel And STructural matERials modelling (FASTER) project.

Contents

Chapter 1

Introduction

Uranium nitride (UN) is a promising alternative nuclear fuel that offers several advantages over traditional fuels such as uranium oxide (UO_2) and metallic uranium. These advantages include higher thermal conductivity and melting point, which could increase the performance and safety margins of a reactor. High thermal conductivity materials help in distributing the heat evenly throughout the fuel, preventing localized hot spots that could lead to fuel damage. The high density of UN would also enable a harder neutron spectrum, which is very beneficial in fast reactors. The long-term performance of irradiated UN fuel is not yet fully understood however, particularly how the thermal conductivity is effected. This is due to the difficulty of performing physical experiments on real irradiated UN. As a result, the possibility of using computational methods instead becomes very attractive. This study investigates the possibility of using first-principles Density Functional Theory (DFT) for calculating transport properties in nuclear materials; in particular the thermal conductivity and electrical resistivity.

The thermal conductivity of a solid is the result of the diffusion of energy carried by electrons and phonons (i.e. crystal vibrations). This diffusion is caused primarily by the collisions between these (quasi)particles. Accurate modeling of the interactions between electrons and phonons, as well as the interactions among phonons themselves, is pivotal for obtaining precise results regarding the material's transport properties. In this work, the relaxation time approximation (RTA) is used to describe the scattering interaction of an electron/phonon with a thermodynamic system of phonons in equilibrium. Furthermore, the relaxation time is assumed to depend on the energy of the electron/phonon, and can be calculated within the framework of DFT and Density Functional Perturbation Theory (DFPT). The Boltzmann transport equation is then applied to each thermodynamic system of electrons and phonons to calculate their respective contribution to the thermal conductivity, from the relaxation time and group velocity of the electrons/phonons.[1] The full theoretical background is treated in the next chapter.

The two most popular software packages for calculating electron-phonon interactions within DFT are Quantum ESPRESSO's 'EPW' code and Abinit's Electron-PHonon driver 'EPH'. Abinit was chosen due to previous experience and the fact that EPH supposedly implements spin-polarized calculations, which would be necessary for magnetic systems like UN. Unfortunately, reliable pseudopotentials have not yet been developed for the actinides in Abinit. Zirconium was therefore chosen as a stepping stone

[1] For the electrical conductivity/resistivity, the Boltzmann transport equation is applied only to the electrons since phonons do not carry charge.

to future studies of Uranium, as Zr forms similar compounds like carbides and nitrides. Zr, ZrC and ZrN are also themselves materials highly relevant in nuclear engineering and reliable experimental reference data is available to verify the calculations against.

One major challenge in using DFT is the large amount of computational resources required to get converged results (all calculations in this work were performed on an HPC cluster), as this limits the size of the system being studied. Because of the periodic nature of crystals it is in principle sufficient to perform the calculation on the irreducible primitive cell containing just a few atoms; corresponding to a perfect crystal with no defects. Defects and disorder in a lattice is known however to have a substantial detrimental effect on thermal conductivity, which have already been experimentally observed for both ZrC and ZrN and is true in general for most alloys. To investigate the effect of defects computationally, a large enough simulation cell must be used to accommodate a sufficient number of atoms.

It is important to first verify the method on simple systems before moving on to more complicated systems like disordered alloys and irradiated nuclear fuel. This study aims at replicating the thermal conductivity and electrical resistivity of perfect crystals of Zr, ZrC, and ZrN, i.e without any defects. It should also be noted that obtaining experimental data for a perfect crystal is tricky due to the difficulty of maintaining a perfect stoichiometric ratio in a sample. This is important to keep in mind when comparing the calculated thermal conductivity with the available reference data as they usually contain some level of impurity.

Chapter 2

Theoretical Background

The thermal conductivity in a solid consist of two contributions: the diffusion of energy carried by electrons and by phonons,

$$\kappa = \kappa_e + \kappa_L.$$

Here, κ_e is the electronic thermal conductivity arising primarily from the interaction between electrons and phonons[1] , and κ_L is the lattice thermal conductivity (LTC) resulting from the interaction between phonons. These contributions have to be computed using similar but different methods.

A brief derivation of density functional theory follows, and how microscopic quantities obtained from DFT can be used in the Boltzmann transport equation to calculate macroscopic transport properties such as thermal conductivity and electrical resistivity.

2.1 Density Functional Theory

DFT is a computational quantum mechanical method used in condensed matter physics, materials science, and chemistry to study the electronic structure of molecules and solids.[19][31] The theory is based on the idea that all properties of a many-body system can be determined from the electron density alone, rather than the wavefunction. To solve the many-body **Schrödinger equation**

$$i\hbar\frac{\partial\Psi}{\partial t} = \hat{H}\Psi,$$

we traditionally look for a wavefunction solution $\Psi(\{\mathbf{r}_i\};t) = \Psi(\mathbf{r}_1, \mathbf{r}_2, \ldots, \mathbf{r}_N; t)$, where $\mathbf{r}_i$ is the position of particle i. To give an example of the memory requirements for storing such a wavefunction of even a small number of electrons, lets suppose we use a grid requiring a modest 10 bytes along each spatial direction. For three dimensions and 8 electrons we have

$$(10^3)^8 \text{ B} = 10^{24} \text{ B} = 1 \text{ Yottabyte !}$$

Thus, solving the Schrödinger equation for Ψ quickly becomes unfeasible. Fortunately, Hohenberg and Kohn proved that all the properties of a system are uniquely determined by the electron ground-state density $n(\mathbf{r})$ alone, a quantity of only $\mathbf{r}$. To derive the DFT

[1] In the absence of phonons, the electron waves would move through the lattice unhindered except for the scattering against lattice defects and impurities.

formalism for finding $n(\mathbf{r})$, we begin with the full Hamiltonian for a many-body system of interacting electrons and nuclei with positions $\mathbf{r}_i$ and $\mathbf{R}_I$ respectively,

$$\hat{H} = -\frac{\hbar^2}{2m_e}\sum_i \nabla_i^2 + \frac{1}{2}\sum_{i\neq j}\frac{e^2}{|\mathbf{r}_i - \mathbf{r}_j|} - \sum_{i,I}\frac{Z_I e^2}{|\mathbf{r}_i - \mathbf{R}_I|} - \sum_I \frac{\hbar^2}{2M_I}\nabla_I^2 + \frac{1}{2}\sum_{I\neq J}\frac{Z_I Z_J e^2}{|\mathbf{R}_I - \mathbf{R}_J|}.$$

Here, Z_I and M_I is the charge and mass of nuclei I. Since the nuclei are slow moving in comparison with the electrons, we consider them stationary (known as the **Born-Oppenheimer approximation**), and the Hamiltonian simplifies to

$$\hat{H} = \hat{T} + \hat{V}_{\text{int}} + \hat{V}_{\text{ext}} + E_{II}, \tag{2.1}$$

where (using Hartree atomic units $\hbar = m_e = e = 4\pi/\epsilon_0 = 1$),

$$\hat{T} = -\sum_i \frac{1}{2}\nabla_i^2, \quad \hat{V}_{\text{int}} = \frac{1}{2}\sum_{i\neq j}\frac{1}{|\mathbf{r}_i - \mathbf{r}_j|}, \quad \hat{V}_{\text{ext}} = -\sum_{i,I}\frac{Z_I}{|\mathbf{r}_i - \mathbf{R}_I|}.$$

The last term E_{II} (the Coulomb potential energy between all the nuclei) is simply a constant. Next, we define the density operator for a system of N electrons,

$$\hat{n}(\mathbf{r}) = \sum_{i=1}^{N}\delta(\mathbf{r} - \mathbf{r}_i),$$

which gives the electron density as[2]

$$\begin{aligned} n(\mathbf{r}) = \langle\Psi|\hat{n}|\Psi\rangle &= \sum_{i=1}^{N}\int d\mathbf{r}_1\cdots d\mathbf{r}_N\,\delta(\mathbf{r}-\mathbf{r}_i)|\Psi(\{\mathbf{r}_j\})|^2 \\ &= \sum_{i=1}^{N}\int d\mathbf{r}_{j\neq i}\,|\Psi(\{\mathbf{r}_{j\neq i}\},\mathbf{r})|^2 \\ &= N\int d\mathbf{r}_{2\ldots N}\,|\Psi(\mathbf{r},\{\mathbf{r}_{2\ldots N}\})|^2, \end{aligned}$$

where exchange of identical particles was performed in the last step. With this expression we can show that the energy from the external potential operator $\hat{V}_{\text{ext}}$ can be expressed as a functional of only $n(\mathbf{r})$,

$$\begin{aligned} E_{\text{ext}}[n] = \langle\Psi|\hat{V}_{\text{ext}}|\Psi\rangle &= \sum_{i,I}\int d\mathbf{r}_1\cdots d\mathbf{r}_N\,\frac{Z_I e^2|\Psi(\mathbf{r}_i,\{\mathbf{r}_{j\neq i}\})|^2}{|\mathbf{r}_i - \mathbf{R}_I|} \\ &= \sum_I Z_I e^2 N\int d\mathbf{r}_1\int d\mathbf{r}_{2\ldots N}\frac{|\Psi(\mathbf{r}_1,\{\mathbf{r}_{2\ldots N}\})|^2}{|\mathbf{r}_1 - \mathbf{R}_I|} \\ &= \int d\mathbf{r}\sum_I\frac{Z_I e^2}{|\mathbf{r}-\mathbf{R}_I|}n(\mathbf{r}) \\ &= \int d\mathbf{r}\,V_{\text{ext}}(\mathbf{r})n(\mathbf{r}) \end{aligned} \tag{2.2}$$

Before continuing with the other operators in $\hat{H}$, a statement of the Hohenberg-Kohn theorems is necessary.

[2] $d\mathbf{r}_{j\neq i} = d\mathbf{r}_1\cdots d\mathbf{r}_{j\neq i}\cdots d\mathbf{r}_N$

2.1.1 The Hohenberg-Kohn Theorems

Theorem 1: If two systems of electrons are confined in potentials $V_{\text{ext}}^{(1)}(\mathbf{r})$ and $V_{\text{ext}}^{(2)}(\mathbf{r})$, respectively, and share the same ground-state density $n_0(\mathbf{r})$, then the difference $V_{\text{ext}}^{(1)} - V_{\text{ext}}^{(2)}$ must be a constant.

Proof: We can construct the full Hamiltonian for each potential, $V_{\text{ext}}^{(1)}(\mathbf{r}) \to \hat{H}_1$, having ground state Ψ_1. Similarly for $V_{\text{ext}}^{(2)}(\mathbf{r}) \to \Psi_2$. Both Ψ_1 and Ψ_2 are assumed to have the same ground-state density $n_0(\mathbf{r})$. Expressed succinctly:

$$V_{\text{ext}}^{(1)}(\mathbf{r}) \to \hat{H}_1 \to \Psi_1 \to n_0(\mathbf{r}) \leftarrow \Psi_2 \leftarrow \hat{H}_2 \leftarrow V_{\text{ext}}^{(2)}(\mathbf{r})$$

Applying the variational principle for the ground-state energy of $\hat{H}_1$ we have

$$E_1 = \langle \Psi_1 | \hat{H}_1 | \Psi_1 \rangle < \langle \Psi_2 | \hat{H}_1 | \Psi_2 \rangle = \langle \Psi_2 | \hat{H}_2 | \Psi_2 \rangle + \langle \Psi_2 | \hat{H}_1 - \hat{H}_2 | \Psi_2 \rangle$$

$$\implies E_1 < E_2 + \int d^3r \left[V_{\text{ext}}^{(1)}(\mathbf{r}) - V_{\text{ext}}^{(2)}(\mathbf{r}) \right] n_0(\mathbf{r})$$

where Eq. (2.2) was used in the last step. The same argument for $\hat{H}_2$ yields similarly,

$$E_2 < E_1 + \int d^3r \left[V_{\text{ext}}^{(2)}(\mathbf{r}) - V_{\text{ext}}^{(1)}(\mathbf{r}) \right] n_0(\mathbf{r})$$

Adding these together,

$$\implies E_1 + E_2 < E_1 + E_2,$$

results in a contradiction! Thus, there cannot be two different potentials having the same n_0 unless they differ by only a constant. Remember: the addition of a constant to $\hat{H}$ yields the same Ψ (only the eigenvalues change) and the inequality becomes an equality above.

■

Corollary 1: Given that the Hamiltonian is fully determined, except for a constant energy shift, it follows that the many-body wavefunctions for all states, including ground and excited states, are also determined. Hence, all properties of a system are entirely determined by the ground-state density $n_0(\mathbf{r})$.

Theorem 2: For any external potential $V_{\text{ext}}(\mathbf{r})$, a functional $E[n]$ of the total energy in terms of the density $n(\mathbf{r})$ can be defined. The minimum value of this functional is the ground-state energy of the system, and is given by the ground-state density, $E[n_0] = \min(E[n])$.

Proof: We have already shown that the energy of the external potential can be written as a functional of n in Eq. (2.2). In general, there is not a one-to-one relationship between the wavefunction and density, $\Psi \to n$. Consider the set of Ψ having the same density n and choose a Ψ that minimizes the total energy from Eq. (2.1),

$$E = \min_{\Psi \to n} \langle \Psi | \hat{H} | \Psi \rangle = \min_{\Psi \to n} \left(\langle \Psi | \hat{T} | \Psi \rangle + \langle \Psi | \hat{V}_{\text{int}} | \Psi \rangle \right) + \int d^3r \, V_{\text{ext}}(\mathbf{r}) n(\mathbf{r}) + E_{II}$$

$$= T[n] + E_{\text{int}}[n] + \int d^3r \, V_{\text{ext}}(\mathbf{r}) n(\mathbf{r}) + E_{II} = E[n]$$

Now consider a specific wavefunction Ψ_1 corresponding to a density $n_1 \neq n_0$. Applying the variational principle

$$E_0 = E[n_0] = \langle \Psi_0 | \hat{H} | \Psi_0 \rangle < \langle \Psi_1 | \hat{H} | \Psi_1 \rangle = E[n_1] = E_1 \qquad \blacksquare$$

Corollary 2: The ground-state energy and density can be determined from the functional $E[n]$ alone.

The only problem is *finding* an explicit expression for the functionals. This was relatively straight forward for the external potential in Eq. (2.2), but for the kinetic operator $\hat{T}$ and interacting potential $\hat{V}_{\text{int}}$ we are not so lucky. This is where the Kohn-Sham auxiliary system comes to the rescue.

2.2 Kohn-Sham DFT

The Kohn-Sham approach, which is the most widely used implementation of DFT, maps the many-body electronic problem onto a set of non-interacting electrons in an effective potential, which is a functional of the electron density. This is accomplished by introducing a set of fictitious non-interacting electrons that move in the same effective potential as the true electrons. The effective potential is obtained by solving a set of self-consistent equations, known as the Kohn-Sham equations.

2.2.1 Non-interacting system

For a system of non-interacting electrons moving in some effective potential $V_{\text{eff}}(\mathbf{r})$ the electrons must obey

$$\left[-\frac{1}{2}\nabla^2 + V_{\text{eff}}(\mathbf{r}) \right] \psi_k(\mathbf{r}) = \varepsilon_k \psi_k(\mathbf{r})$$

A wavefunction obeying the full Hamiltonian and anti-symmetrization requirement is the **Slater determinant**

$$\Psi(\mathbf{r}_1, \mathbf{r}_2, \ldots, \mathbf{r}_N) = \frac{1}{\sqrt{N!}} \begin{vmatrix} \psi_1(\mathbf{r}_1) & \psi_2(\mathbf{r}_1) & \cdots & \psi_N(\mathbf{r}_1) \\ \psi_1(\mathbf{r}_2) & \psi_2(\mathbf{r}_2) & \cdots & \psi_N(\mathbf{r}_2) \\ \vdots & \vdots & \ddots & \vdots \\ \psi_1(\mathbf{r}_N) & \psi_2(\mathbf{r}_N) & \cdots & \psi_N(\mathbf{r}_N) \end{vmatrix}$$

This has the useful property that the electron density can be expressed as

$$n(\mathbf{r}) = \sum_{i=1}^{N} |\psi_i(\mathbf{r})|^2 \tag{2.3}$$

We make the ansatz that the energy functional can be written as

$$E[n] = T_s[n] + \underbrace{\frac{1}{2} \int d\mathbf{r} d\mathbf{r}' \, \frac{n(\mathbf{r}) n(\mathbf{r}')}{|\mathbf{r} - \mathbf{r}'|}}_{E_{\text{Hartree}}} + \int d\mathbf{r} \, V_{\text{ext}}(\mathbf{r}) n(\mathbf{r}) + E_{\text{xc}}[n] \tag{2.4}$$

Here we've replaced $\hat{T}$ in Eq. (2.1) with the independent-particle kinetic operator

$$T_s = -\frac{1}{2}\sum \langle \psi_i | \nabla^2 | \psi_i \rangle \,, \tag{2.5}$$

and $\hat{V}_{\text{int}}$ with the classical interacting Coulomb potential of the electron density, $E_{\text{Hartree}}[n]$. Note that T_s must also be a functional of n by Hohenberg-Kohn's 2nd theorem, even though it is written in terms of the individual orbitals. The exchange–correlation energy term E_{xc} contains all the unaccounted many-body effects of exchange and correlation. Comparing Eq. (2.1) and (2.4) we see that

$$E_{\text{xc}}[n] = \langle \hat{T} \rangle - T_s[n] + \langle \hat{V}_{\text{int}} \rangle - E_{\text{Hartree}}[n]$$

is simply the difference in kinetic and internal interaction energies between the true many-body system and the fictitious independent-particle system. The exact form of $E_{\text{xc}}[n]$ is unknown but valid approximations are given below.

We now apply the method of Lagrange multipliers to Eq. (2.4) with the constraint that the total number of electrons must equal N,

$$E[n] - \varepsilon(\int d\mathbf{r}\, n(\mathbf{r}) - N) = 0.$$

Variation of this equation with respect to ψ_i^* then gives

$$\frac{\delta T_s}{\delta \psi_i^*} + \left[\frac{\delta E_{\text{ext}}}{\delta n} + \frac{\delta E_{\text{Hartree}}}{\delta n} + \frac{\delta E_{\text{xc}}}{\delta n}\right]\frac{\delta n}{\delta \psi_i^*} - \varepsilon_i \frac{\delta n}{\delta \psi_i^*} = 0 \tag{2.6}$$

From Eq. (2.5) and Eq. (2.3) we find

$$\frac{\delta T_s}{\delta \psi_i^*} = -\frac{1}{2}\nabla^2 \psi_i, \quad \frac{\delta n}{\delta \psi_i^*} = \psi_i.$$

Substituting these expressions back in Eq. (2.6), we arrive at the Kohn-Sham auxiliary system

$$\left(-\frac{1}{2}\nabla^2 + V_{\text{eff}} - \varepsilon_i\right)\psi_i = 0,$$
$$V_{\text{eff}} = \frac{\delta E_{\text{ext}}}{\delta n} + \frac{\delta E_{\text{Hartree}}}{\delta n} + \frac{\delta E_{\text{xc}}}{\delta n}.$$

The Kohn-Sham equations are solved iteratively, starting from an initial guess for the electron density. In each iteration, the electron density is used to construct the effective potential, which in turn is used to solve for the wavefunctions of the fictitious electrons. The resulting electron density is then compared with the initial guess, and the procedure is repeated until self-consistency is achieved, as illustrated in Fig. 2.1.

2.2.2 Local Density Approximation

The simplest approximation for E_{xc} is the LDA, which is based on the interacting homogenous electron gas (HEG) model. It can be shown from the Thomas-Fermi-Dirac model for an HEG that the exchange energy per electron is

$$\epsilon_x = -\frac{3k_F}{4\pi} = -\frac{3}{4}\left(\frac{3}{\pi}n\right)^{1/3} \implies E_x[n] = \int d\mathbf{r}\, \epsilon_x n(\mathbf{r}) = C_x \int d\mathbf{r}[n(\mathbf{r})]^{4/3}$$

The derivation for the energy functional for the correlation energy $E_c[n]$ is beyond this text (actually only possible in the high/low density limit) and general expressions are usually obtained via quantum Monte-Carlo simulations.[19][31]

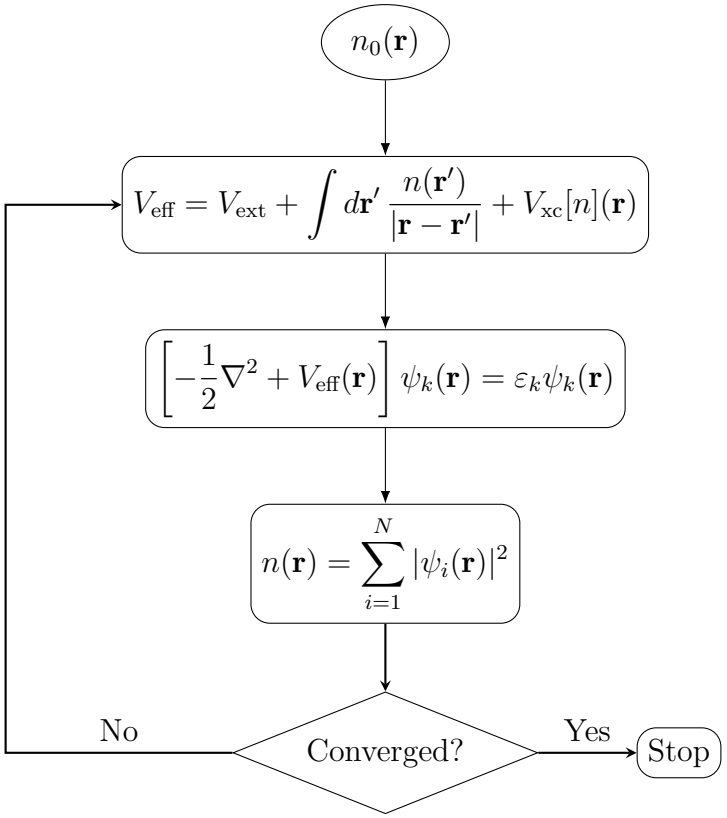

Figure 2.1: The Kohn-Sham self-consistency cycle.

2.2.3 Generalized Gradient Approximation

A natural improvement to the LDA is to include the gradients of n,

$$E_{\text{xc}}^{\text{GGA}}[n] = \int d\mathbf{r} F(n, \nabla n),$$

for some functional F. Many such functionals have been developed, though this work use exclusively the GGA by Perdew-Burke-Ernzerhof for solids, PBEsol.[23][24]

2.2.4 Periodic Solids

If the electrons are moving in a periodic potential $V_{\text{eff}}(\mathbf{r} + \mathbf{T}) = V_{\text{eff}}(\mathbf{r})$ then according to Bloch's theorem the single electron wavefunctions can be written as

$$\psi_{n\mathbf{k}}(\mathbf{r}) = e^{i\mathbf{k}\cdot\mathbf{r}} u_{n\mathbf{k}}(\mathbf{r}),$$

where $u_{n\mathbf{k}}(\mathbf{r} + \mathbf{T}) = u_{n\mathbf{k}}(\mathbf{r})$ is a periodic function (n denotes the band index in this context). Since the number of atoms in a solid is for all practical concerns infinite, the possible values of $\mathbf{k}$ becomes a continuum and the summation in Eq. (2.3) becomes an integration over the Brillouin zone and a summation over bands (under the condition that the electron density integrates to the total number of electrons in the primitive cell),[3]

$$n(\mathbf{r}) = \sum_n \int_{\text{BZ}} d\mathbf{k}\, f_{n\mathbf{k}} |\psi_{n\mathbf{k}}(\mathbf{r})|^2.$$

[3]Using notation $\int d\mathbf{k} = \int \frac{d^3k}{(2\pi)^3}$. In particular, $\int_{\text{BZ}} d\mathbf{k} = \frac{1}{\Omega_{\text{p}}}$, where Ω_{p} is the volume of the primitive cell.

A smearing function $f_{n\mathbf{k}}(T)$ is introduced to ease convergence and avoid numerical issues related to the finite sampling of $\mathbf{k}$-points (for numerical integration) in the BZ. If $f_{n\mathbf{k}}(T)$ is the Fermi-Dirac distribution, then $T = 0$ would result in a step function. It is important to remember that DFT is a ground-state theory meaning the true charge density correspond to $T = 0$, but since such low value might require a very large number of $\mathbf{k}$-points, T must be considered a convergence parameter. Note that the smearing function f does not necessarily need to be the Fermi-Dirac distribution; in fact most of the time various schemes of Gaussian smearing are used as they are more efficient.[19]

2.2.5 Pseudopotentials

Several schemes exists for representing the external potential V_{ext} in periodic solids. The fact that only the valence electrons are involved in chemical bonding can be exploited to reduce the number of explicitly treated electrons in the primitive cell. Pseudopotentials are constructed by replacing the core electrons with an effective potential that reproduces the behavior of the core electrons, while leaving the valence electrons largely unchanged. The most commonly used scheme is the norm-conserving pseudopotential (NCPP), which is designed to preserve the norm of the wave function, i.e., the probability of finding an electron in a given region of space. Other types of pseudopotentials include ultrasoft pseudopotentials (USPP) and projector-augmented wave (PAW) pseudopotentials.

2.3 Density Functional Perturbation Theory

DFPT is a method to efficiently calculate the response of a system to perturbations such as phonons, electric and magnetic fields, or strains. The DFPT formalism can be derived by applying first-order perturbation theory to the Kohn-Sham system. If we let $\Delta\psi_i$ denote the first-order correction to orbital ψ_i then[6]

$$(H_{\text{KS}} - \varepsilon_i)\,|\Delta\psi_i\rangle = -(\Delta V_{\text{eff}} - \Delta\varepsilon_i)\,|\psi_i\rangle\,,$$

where $\Delta\varepsilon_i = \langle\psi_i|\Delta V_{\text{eff}}|\psi_i\rangle$. The perturbation of the effective KS potential is

$$\begin{aligned}\Delta V_{\text{eff}} &= \Delta V_{\text{ext}} + \int d\mathbf{r}'\,\frac{\Delta n(\mathbf{r}')}{|\mathbf{r}-\mathbf{r}'|} + \frac{\delta V_{\text{xc}}[n](\mathbf{r})}{\delta n}\Delta n,\\ \Delta n(\mathbf{r}) &= 2\,\text{Re}\sum \psi_i^*(\mathbf{r})\Delta\psi_i(\mathbf{r}).\end{aligned}$$

This forms a set of self-consistent equations that can be solved similarly to the Kohn-Sham system.[19]

2.4 Boltzmann Transport Theory

The Boltzmann transport equation (BTE) describes the statistical behavior of a non-equilibrium thermodynamic system. It allows for the calculation of macroscopic properties such as mobility, diffusion coefficient, and conductivity, in terms of microscopic properties.[2][27]

At equilibrium the distribution function for an electron gas is simply the Fermi-Dirac distribution

$$f^0(\mathbf{r},\mathbf{k}) = \frac{1}{\exp\left(\dfrac{\varepsilon(\mathbf{k})-\mu(\mathbf{r})}{k_B T(\mathbf{r})}\right)+1}.$$

Although collisions will cause electrons to move between different $\mathbf{k}$-states, there is no net redistribution from the Fermi-Dirac function as long as no external forces are present. To determine the distribution as a result of external disturbances, we let $f_{n\sigma}(\mathbf{r},\mathbf{k},t)$ denote the local concentration of electrons in state $\mathbf{k}$ in the neighborhood of $\mathbf{r}$, where the band number n and spin σ is included for completion. Boltzmann's method entails accounting for three different reasons for the change in electron distribution in $\mathbf{k}$-space and $\mathbf{r}$-space:

- The diffusion of electrons.
- The motion due to external forces, i.e. $\hbar d\mathbf{k}/dt = \mathbf{F}_{\text{ext}}$.
- Scattering of electrons, causing them to move from one $\mathbf{k}$-state to another.

All of these contributions can be accounted for by applying the continuity equation to the distribution function f with generalized coordinates $\mathbf{u} = (\dot{\mathbf{r}}, \dot{\mathbf{k}})$ and $\nabla = (\nabla_{\mathbf{r}}, \nabla_{\mathbf{k}})$. At any point in $\mathbf{u}$, a change in f must equal the net flow through that point plus any change due to collisions,

$$\frac{\partial f}{\partial t} + \nabla\cdot(\mathbf{u}f) = \left(\frac{\partial f}{\partial t}\right)_{\text{coll}}. \tag{2.7}$$

The dynamics of a wavepacket in a solid can be described by the semiclassical equations

$$\begin{aligned}\dot{\mathbf{r}} &= \mathbf{v} = \frac{1}{\hbar}\frac{\partial \varepsilon_{\mathbf{k}}}{\partial \mathbf{k}},\\ \dot{\mathbf{k}} &= -\frac{e}{\hbar}\left[\mathbf{E}(\mathbf{r},t) + \mathbf{v}(\mathbf{k})\times\mathbf{B}\right].\end{aligned} \tag{2.8}$$

From this we have $\nabla\cdot\mathbf{u} = 0$, assuming ε is a function of $\mathbf{k}$ alone and does not vary with $\mathbf{r}$. In other words phase-space flows are incompressible. Eq. (2.7) then simplifies to

$$\frac{\partial f}{\partial t} + \dot{\mathbf{r}}\cdot\frac{\partial f}{\partial \mathbf{r}} + \dot{\mathbf{k}}\cdot\frac{\partial f}{\partial \mathbf{k}} = \left(\frac{\partial f}{\partial t}\right)_{\text{coll}}. \tag{2.9}$$

We define δf as the deviation from equilibrium f^0,

$$f(\mathbf{r},\mathbf{k},t) = f^0(\mathbf{r},\mathbf{k}) + \delta f(\mathbf{r},\mathbf{k},t). \tag{2.10}$$

The goal is to express the Boltzmann transport equation in terms of δf, since it is this deviation which is responsible for any net transport of energy/particles. Inserting Eq. (2.10) in (2.9), and after a tedious bit of simplification we arrive at

$$\frac{\partial \delta f}{\partial t} + \mathbf{v}\cdot\nabla_r \delta f - \frac{e}{\hbar}\left[\mathbf{E}+\mathbf{v}\times\mathbf{B}\right]\cdot\frac{\partial \delta f}{\partial \mathbf{k}} - \mathbf{v}\cdot\left[\underbrace{e\mathbf{E}+\nabla_r\mu}_{e\boldsymbol{\mathcal{E}}} + \frac{\varepsilon-\mu}{T}\nabla_r T\right]\frac{\partial f^0}{\partial \varepsilon} = \left(\frac{\partial f}{\partial t}\right)_{\text{coll}},$$

Here, the electromotive field $\boldsymbol{\mathcal{E}}$ can be written as the gradient of the electrochemical potential: $\boldsymbol{\mathcal{E}} = -\nabla(\phi - \mu/e)$. We can linearize this equation by assuming the gradients of δf are small, which they should be near equilibrium:

$$\frac{\partial \delta f}{\partial t} - \mathbf{v} \cdot \left[e\boldsymbol{\mathcal{E}} + \frac{\varepsilon - \mu}{T} \nabla_r T \right] \frac{\partial f^0}{\partial \varepsilon} = \left(\frac{\partial f}{\partial t} \right)_{\text{coll}} \tag{2.11}$$

This is the linearized BTE. To continue we need some expression for the collision term, the simplest being the **relaxation time approximation** (RTA):

$$\left(\frac{\partial f}{\partial t} \right)_{\text{coll}} = -\frac{f - f^0}{\tau} = -\frac{\delta f}{\tau}, \tag{2.12}$$

for some time-constant τ. In the absence of electric/magnetic fields and temperature gradients, any disturbance will decay according to

$$\frac{\partial \delta f}{\partial t} = -\frac{\delta f}{\tau} \implies \delta f = \delta f(0) e^{-t/\tau}.$$

Combining Eq. (2.11) and (2.12) we get in the steady state

$$\delta f = \tau \mathbf{v} \cdot \left[e\boldsymbol{\mathcal{E}} + \frac{\varepsilon - \mu}{T} \nabla_r T \right] \frac{\partial f^0}{\partial \varepsilon}. \tag{2.13}$$

To obtain expressions for the electrical and thermal conductivity we begin by noting that the current density can be expressed by[4]

$$\boldsymbol{j}(\mathbf{r}, t) = -e \sum_{n,\sigma} \int_{\text{BZ}} d\mathbf{k}\, f_{n\sigma}(\mathbf{r}, \mathbf{k}, t) \mathbf{v}_n(\mathbf{k}) = -e \int_{\text{BZ}} d\mathbf{k}\, \mathbf{v} \delta f,$$

where the summation over band and spin is implicit on the right-hand side. Only the deviation from equilibrium δf contributes to the current. Next, we consider a region of the solid with fixed volume ΔV. By the first law of thermodynamics (conservation of energy) we have

$$T\Delta S = \Delta E - \mu \Delta N.$$

Dividing by ΔV yields

$$dq = T ds = d\varepsilon - \mu dn,$$

where q is the heat density, s the entropy density, ε the energy density, and n the number density. This can also be written in terms of currents,

$$\boldsymbol{j}_q = T \boldsymbol{j}_s = \boldsymbol{j}_\varepsilon - \mu \boldsymbol{j}_n,$$

where $\boldsymbol{j}_n = \boldsymbol{j}/(-e)$, and $\boldsymbol{j} = -ne\mathbf{v} = \sigma \boldsymbol{\mathcal{E}}$. The energy current density is given by

$$\boldsymbol{j}_\varepsilon = \int_{\text{BZ}} d\mathbf{k}\, \varepsilon \mathbf{v} \delta f.$$

We can derive an expression for the heat current in terms of the other currents as

$$\boldsymbol{j}_q = T \boldsymbol{j}_s = \boldsymbol{j}_\varepsilon + \frac{\mu}{e} \boldsymbol{j} = \int_{\text{BZ}} d\mathbf{k}\, (\varepsilon - \mu) \mathbf{v} \delta f$$

[4]Using notation $\int d\mathbf{k} = \int \frac{d^3k}{(2\pi)^3}$

Expressing the charge and heat currents in terms of the electromotive field and temperature gradient which drive them, and making use of Onsager's reciprocal relations we have[3]

$$\begin{aligned} \boldsymbol{j} &= -e\int_{\mathrm{BZ}} d\mathbf{k}\,\mathbf{v}\delta f \quad &= \quad \mathcal{L}^{(0)}\boldsymbol{\mathcal{E}} - \frac{\mathcal{L}^{(1)}}{eT}(-\nabla T) \\ \boldsymbol{j}_q &= \int_{\mathrm{BZ}} d\mathbf{k}\,(\varepsilon-\mu)\mathbf{v}\delta f = -\frac{\mathcal{L}^{(1)}}{e}\boldsymbol{\mathcal{E}} + \frac{\mathcal{L}^{(2)}}{e^2T}(-\nabla T) \end{aligned} \tag{2.14}$$

On the right-hand side we include the factors T and $-e$ to get a unified expression for $\mathcal{L}^{(m)}$ in the next step. Inserting δf from the linearized BTE, Eq. (2.13), and identifying terms we obtain an expression for the **generalized transport coefficients**

$$\mathcal{L}^{(m)} = e^2\sum_n \int_{\mathrm{BZ}} d\mathbf{k}\,\tau_{n\mathbf{k}}\cdot(\varepsilon_{n\mathbf{k}}-\mu)^m \mathbf{v}_{n\mathbf{k}}\otimes\mathbf{v}_{n\mathbf{k}}\left(-\frac{\partial f^0}{\partial\varepsilon}\right)$$

The full notation is given here, including the dependence on $n\mathbf{k}$ for τ and $\mathbf{v}$ (spin is implicit in n). Note that the outer product implies $\mathcal{L}^{(m)}$ is a second order tensor.

From Eq. (2.14) we can also identify the electrical conductivity, the electronic contribution to the thermal conductivity, the Peltier coefficient, and Seebeck coefficient as

$$\sigma = \mathcal{L}^{(0)}, \tag{2.15}$$

$$\kappa_e = \frac{1}{e^2T}\left[\frac{(\mathcal{L}^{(1)})^2}{\mathcal{L}^{(0)}} - \mathcal{L}^{(2)}\right], \tag{2.16}$$

$$\Pi = -\frac{\mathcal{L}^{(1)}}{e\mathcal{L}^{(0)}}, \tag{2.17}$$

$$S = -\frac{1}{eT}\frac{\mathcal{L}^{(1)}}{\mathcal{L}^{(0)}}. \tag{2.18}$$

We have thus managed to express macroscopic transport properties in terms of microscopic quantities. The velocity $\mathbf{v}_{n\mathbf{k}}$ can be obtained via interpolation of the band structure from DFT, and the relaxation time $\tau_{n\mathbf{k}}$ from the interaction between electrons and phonons given below.

2.5 Relaxation time approximation

In solids, phonons can interact with electrons, leading to scattering events that perturb the distribution function f. The relaxation time approximation was introduced in Eq. (2.12) where the relaxation time τ describes how fast a perturbation returns to equilibrium.

There are several ways to approximate τ, the simplest is taking it to be a constant (known as CRTA) independent of the electron energy $\varepsilon_{n\mathbf{k}}$. This approach has had some success where τ might be fitted to experimental data (such as resistivity ρ) via the Drude model,[10]

$$\tau_D = \frac{m_e}{\rho n e^2}.$$

For the Seebeck and Peltier coefficients in Eq. (2.18) and (2.17) a constant τ would even cancel out. In cases when we don't have experimental data (ρ is usually the unknown

property we are trying to calculate!) this approach can't be applied. Furthermore, electron-phonon interaction is a complicated phenomena and τ usually varies greatly with electron energy. An excellent example of the inadequacies of CRTA can be found in Ref. [36], where the Seebeck coefficient of Lithium is calculated using different approximations for τ.

A fully first-principle approach becomes necessary. One such method is the self-energy relaxation time approximation (SERTA) which takes into account the energy an electron has when interacting with its environment. The derivation of τ within SERTA is much too lengthy to repeat here so I will simply refer to an excellent treatise on the subject in Ref. [4]. The main results are

$$\begin{aligned}\frac{1}{\tau_{n\mathbf{k}}} = 2 \lim_{\eta\to 0^+} \mathrm{Im}\{\Sigma^{\mathrm{FM}}_{n\mathbf{k}}(\varepsilon_{n\mathbf{k}})\} = \; & \frac{2\pi}{\hbar}\sum_{m,\nu}\int_{\mathrm{BZ}}\frac{d\mathbf{q}}{\Omega_{\mathrm{BZ}}}|g_{mn\nu}(\mathbf{k},\mathbf{q})|^2 \\ & \times[(1-f_{m\mathbf{k}+\mathbf{q}}+n_{\mathbf{q}\nu})\delta(\varepsilon_{n\mathbf{k}}-\hbar\omega_{\mathbf{q}\nu}-\varepsilon_{m\mathbf{k}+\mathbf{q}}) \\ & \quad +(f_{m\mathbf{k}+\mathbf{q}}+n_{\mathbf{q}\nu})\delta(\varepsilon_{n\mathbf{k}}+\hbar\omega_{\mathbf{q}\nu}-\varepsilon_{m\mathbf{k}+\mathbf{q}})]\,,\end{aligned} \tag{2.19}$$

where $\Sigma^{\mathrm{FM}}_{n\mathbf{k}}$ is the Fan-Migdal term of the electron-phonon self-energy, Ω_{BZ} is the volume of the BZ, $n_{\mathbf{q}\nu}$ is the Bose-Einstein distribution, and the electron-phonon matrix elements are given by

$$g_{mn\nu}(\mathbf{k},\mathbf{q}) = \langle\psi_{m\mathbf{k}+\mathbf{q}}|\Delta_{\mathbf{q}\nu}V^{\mathrm{KS}}|\psi_{n\mathbf{k}}\rangle\,, \tag{2.20}$$

where $\Delta_{\mathbf{q}\nu}V^{\mathrm{KS}}$ is the first-order variation of the self-consistent KS potential induced by the phonon mode $\mathbf{q}\nu$, which can be obtained from DFPT calculations.

Another method implemented in Abinit is the momentum relaxation time approximation (MRTA), where the back-scattering is included,

$$\begin{aligned}\frac{1}{\tau_{n\mathbf{k}}} = \; & \frac{2\pi}{\hbar}\sum_{m,\nu}\int_{\mathrm{BZ}}\frac{d\mathbf{q}}{\Omega_{\mathrm{BZ}}}|g_{mn\nu}(\mathbf{k},\mathbf{q})|^2\left(1-\frac{\mathbf{v}_{n\mathbf{k}}\cdot\mathbf{v}_{n\mathbf{k}+\mathbf{q}}}{|\mathbf{v}_{n\mathbf{k}}|^2}\right) \\ & \times[(1-f_{m\mathbf{k}+\mathbf{q}}+n_{\mathbf{q}\nu})\delta(\varepsilon_{n\mathbf{k}}-\hbar\omega_{\mathbf{q}\nu}-\varepsilon_{m\mathbf{k}+\mathbf{q}}) \\ & \quad +(f_{m\mathbf{k}+\mathbf{q}}+n_{\mathbf{q}\nu})\delta(\varepsilon_{n\mathbf{k}}+\hbar\omega_{\mathbf{q}\nu}-\varepsilon_{m\mathbf{k}+\mathbf{q}})]\,.\end{aligned} \tag{2.21}$$

Though similar results are usually obtained from SERTA and MRTA, sometimes the transport properties differs greatly between the two.

2.6 Lattice thermal conductivity

The Boltzmann transport equation and relaxation time approximation can similarly be applied to a system of interacting phonons, where the Fermi-Dirac distribution is replaced by the Bose-Einstein distribution. This is the method implemented in the Phono3py package. The main results are:[32][29][37]

$$\kappa_L = \frac{1}{NV_0}\sum_{\lambda} C_\lambda \mathbf{v}_\lambda \otimes \mathbf{v}_\lambda \tau^{\mathrm{SMRT}}_\lambda, \tag{2.22}$$

where N is the number of unit cells in a supercell crystal, V_0 is the volume of the unit cell, $\mathbf{v}_\lambda$ is the group velocity for phonons in mode λ, and C_λ is the mode dependent heat capacity,

$$C_\lambda = k_{\mathrm{B}}\left(\frac{\hbar\omega_\lambda}{k_{\mathrm{B}}T}\right)^2\frac{\exp\left(\hbar\omega_\lambda/k_{\mathrm{B}}T\right)}{[\exp\left(\hbar\omega_\lambda/k_{\mathrm{B}}T\right)-1]^2}. \tag{2.23}$$

Here, ω_λ is the phonon frequency. $\tau_\lambda^{\mathrm{SMRT}}$ is the single-mode relaxation time (SMRT) which is the equivalent of SERTA for electrons. In SMRT the relaxation time of phonons is calculated under the assumption that all other phonon modes are in equilibrium,

$$\begin{aligned}\frac{1}{\tau_\lambda^{\mathrm{SMRT}}} = 2\Gamma_\lambda(\omega) = \frac{36\pi}{\hbar^2}\sum_{\lambda'\lambda''}|\Phi_{-\lambda\lambda'\lambda''}|^2\{(n_{\lambda'}+n_{\lambda''}+1)\delta(\omega-\omega_{\lambda'}-\omega_{\lambda''}) \\ +(n_{\lambda'}-n_{\lambda''})[\delta(\omega+\omega_{\lambda'}-\omega_{\lambda''})-\delta(\omega-\omega_{\lambda'}+\omega_{\lambda''})]\}\end{aligned} \tag{2.24}$$

This expression has a similar form to Eq. (2.19). Here, $\Gamma_\lambda(\omega)$ is the imaginary part of the phonon self energy, and $\Phi_{-\lambda\lambda'\lambda''}$ is the interaction strength between the three phonons λ, λ', and λ'' involved in the scattering. It is the analogue to the electron-phonon matrix elements in Eq. (2.20) and can be calculated from the third-order force constants.

Higher order force constants

If the atomic potential were harmonic no two phonons could interact with each other and there would be no thermal diffusion in the lattice. It is only thanks to higher order force constants (primarily third-order) that phonons can interact at all.[13] Most DFPT codes only calculates the harmonic force constants, so to access higher orders one has to resort to finite difference methods, which is what the Phono3py package does.

It was found that Phono3py overestimates the lattice thermal conductivity for low/intermediate temperatures. Phono3py is written primarily with semiconductors and insulators in mind, systems where the interaction between electrons and phonons can be neglected. But for metals this interaction should be taken into account, where the total scattering rate of phonons can be expressed using Matthiessen's rule as[22]

$$\frac{1}{\tau_{\mathbf{q}\nu}^{\mathrm{p}}} = \frac{1}{\tau_{\mathbf{q}\nu}^{\mathrm{pp}}} + \frac{1}{\tau_{\mathbf{q}\nu}^{\mathrm{pe}}}. \tag{2.25}$$

Phono3py only calculates the first term via SMRT from Eq. (2.24). The second term should be possible to calculate from SERTA in Eq. (2.19). From literature, the equivalent expression for the relaxation time for phonons is[33][4]

$$\frac{1}{\tau_{\mathbf{q}\nu}^{\mathrm{pe}}} = \frac{2\pi}{\hbar}2\sum_{mn}\int_{\mathrm{BZ}}\frac{d\mathbf{k}}{\Omega_{\mathrm{BZ}}}|g_{mn\nu}(\mathbf{k},\mathbf{q})|^2(f_{n\mathbf{k}}-f_{m\mathbf{k}+\mathbf{q}})\times\delta(\varepsilon_{m\mathbf{k}+\mathbf{q}}-\varepsilon_{n\mathbf{k}}-\hbar\omega_{\mathbf{q}\nu}) \tag{2.26}$$

It has been shown that for Cu, the electron-phonon scattering rate dominates for temperatures < 100 K and the phonon-phonon scattering rate dominates for $T > 100$ K.[17] This is not expected to be true in general but is thought to be dependent on the specific electronic structure of a material. It was not possible within the scope of this project to implement Eq. (2.26) in Abinit/phono3py, and the lack of $\tau_{\mathbf{q}\nu}^{\mathrm{pe}}$ should be considered a source of error.

2.7 Wiedemann-Franz law

This is an empirical law which states that the ratio of κ_e and σ is proportional to the temperature in a free-electron metal,[13]

$$\frac{\kappa_e}{\sigma} = LT,$$

where the Lorenz number L can be theoretically derived from the Drude model as

$$L = \frac{\pi^2}{3}\left(\frac{k_\mathrm{B}}{e}\right)^2 = 2.44 \cdot 10^{-8}\ \mathrm{V^2K^{-2}}.$$

Wiedemann-Franz law also states that κ_e and σ are expected to be highly correlated, meaning they're both in a sense a measure of the same quantity. This fact is useful when comparing model with experimental data since a good agreement with σ will naturally also be in good agreement with κ_e. From the expression for σ and κ_e in Eq. (2.15) and (2.16), it is not obvious however that WF-law follows from the generalized transport coefficients. Indeed, deviations from WF-law does occur as shown in Ref. [17].

2.8 The effect of disorder on resistivity

In general, a disordered alloy have a higher resistivity than an ordered alloy because of the greater number of defects and imperfections for the electrons to scatter against. In an ordered alloy, the atoms are arranged in a regular pattern, which allows electrons to move through the material with less resistance. In an alloy such as $\mathrm{Cu}_x\mathrm{Au}_{1-x}$, certain values of x results in a stoichiometric ratio such that an exact number of atoms fit in a primitive cell, creating an ordered lattice. For such compositions the resistivity is significantly decreased, as illustrated in Fig. 2.1.[13] This is important to keep in mind when comparing calculations with experimental data. A DFT calculation of the primitive cell for ZrN would represent a perfect crystal without any defects. Experimental data on the other hand will always contain impurities, porosity and have an inexact stoichiometric ratio.

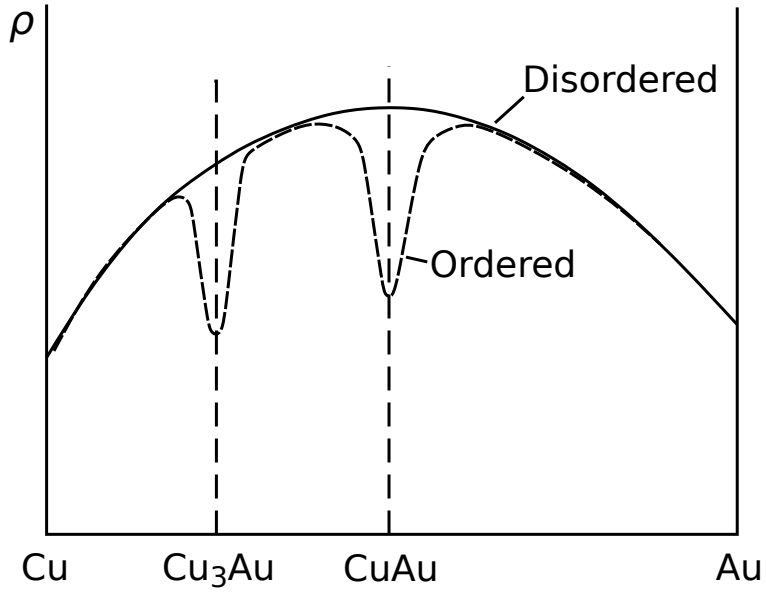

Figure 2.1: Qualitative behaviour for resistivity in ordered/disordered Cu-Au alloy systems.

Many solids can exist in multiple stable crystal structures, called polymorphs, which have different physical and chemical properties. A solid may undergo a solid-solid phase transition to another structure when subjected to a different temperature and pressure. It

is important to check that the correct crystal structure is used when performing transport calculations in a temperature range of interest. For example, the phase diagram of Zr in Fig. 2.2 suggest that the hcp structure should be used between 0 and 1130 K, and bcc from 1130 K to the melting point.

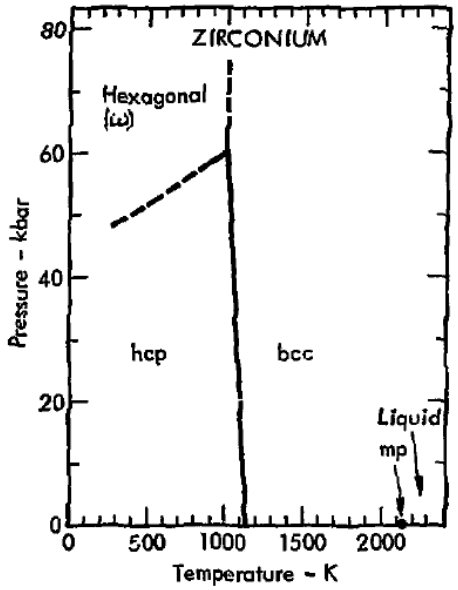

Figure 2.2: Phase diagram for Zirconium. (D.A. Young, *Phase diagrams of the elements*, 1975, Public Domain)

Chapter 3

Methods

Software used

Abinit is a software package implementing the Kohn-Sham DFT formalism, and many of the advanced techniques such as DFPT and many-body Green's functions (GW and DMFT). It is one of the few DFT codes capable of performing electron-phonon interaction calculations via its Electron-PHonon (EPH) driver.[5][18]

AbiPy is a python library for interfacing with Abinit and analyzing output files. It provides tools to generate input files and workflows, as well as submitting calculations on high-performance computing clusters.

Pseudopotentials from the **PseudoDojo** project was used for Abinit. Primarily the norm-conserving semi-relativistic (ONCVPSP v.0.4.1) PBEsol potentials for EPH calculations. PAW PBEsol potentials were used for LTC calculations with Phono3py.[35][8]

Phono3py is a software package for calculating phonon-phonon interaction using the frozen-phonon supercell method. It is capable of calculating force constants up to third-order which is necessary for the computation of the lattice thermal conductivity. Phono3py requires the use of an external force calculator and can interface with most of the widely used DFT codes, including Abinit and VASP.

VASP is another DFT code which was primarily used when calculating the lattice thermal conductivity with phono3py.[15][14][16]

3.1 Electronic transport properties

An initial SCF calculation[1] is performed on a relatively coarse **k**-grid, which is used as input for a set of DFPT calculations for phonon perturbations on a **q**-grid. Abinit is able to detect the symmetry of the system to reduce the number of **q**-points to only the irreducible atomic perturbations. The **q**-grid must be commensurate with the **k**-grid, and was for simplicity always set equal to each other.

[1] A self-consistent field (SCF) calculation refers to the iterative process of finding a self-consistent electron density that minimizes the total energy of the system according to the Kohn-Sham equations, as illustrated in Fig. 2.1.

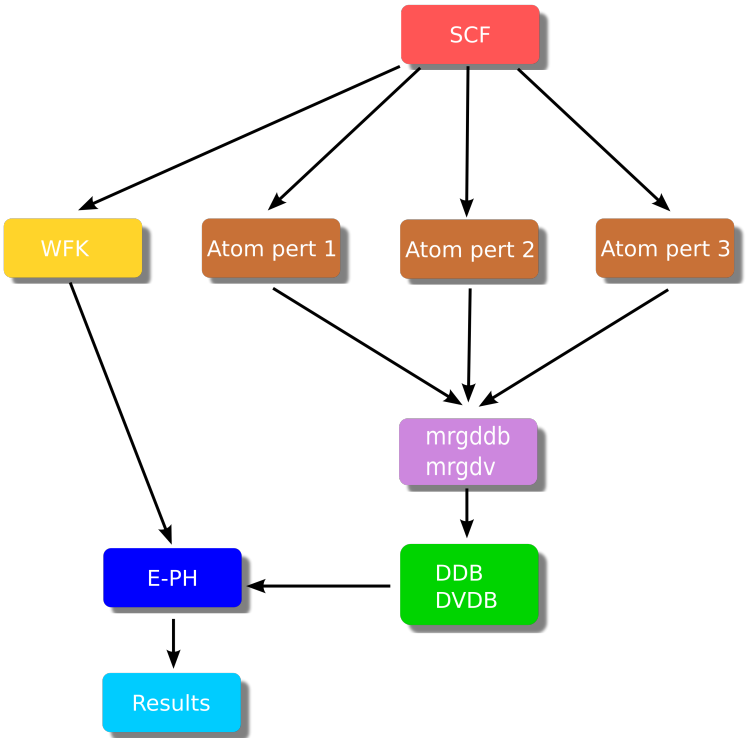

Figure 3.1: Abinit EPH calculation workflow.

Each DFPT run produces a partial DDB file as well as POT files containing the first-order derivative of the KS potential. The Derivative DataBase (DDB) contains a list of derivatives of the total energy with respect to three kind of perturbations: phonons, electric field and stresses. When all the DFPT runs are completed, the partial POT files are merged with the `mrgdv` utility to produce a single DVDB file (Derivatives of $V(\mathbf{r})$ DataBase). The partial DDB files are similarly merged with `mrgddb` into a single DDB file.

The DFPT calculations are performed on a relatively coarse **q**-grid to improve efficiency, and is interpolated on a denser grid in the EPH calculations. The **k**-grid is likewise interpolated on a denser grid in a NSCF calculation[2]. After the **k**- and **q**-grid have been interpolated, the relaxation times and generalized transport coefficients are calculated to finally give the transport properties. The results are given in both SERTA and MRTA. The whole process is schematically shown in Fig. 3.1, and the specific AbiPy workflow implementation is displayed in Fig. 3.2.

3.2 Lattice thermal conductivity

The conventional cell was made to relax with a relatively high number k-points. Phono3py was used to generate supercell displacement sets for each atom within a nearest-neighbor cutoff distance. VASP then calculates the forces within each displacement set. To increase precision, the projection operators were set to be evaluated in reciprocal space; and an additional support grid were used for the evaluation of the augmentation charges:

[2]A non-self-consistent field (NSCF) calculation is performed on a fixed electronic structure obtained from a previously converged SCF calculation.

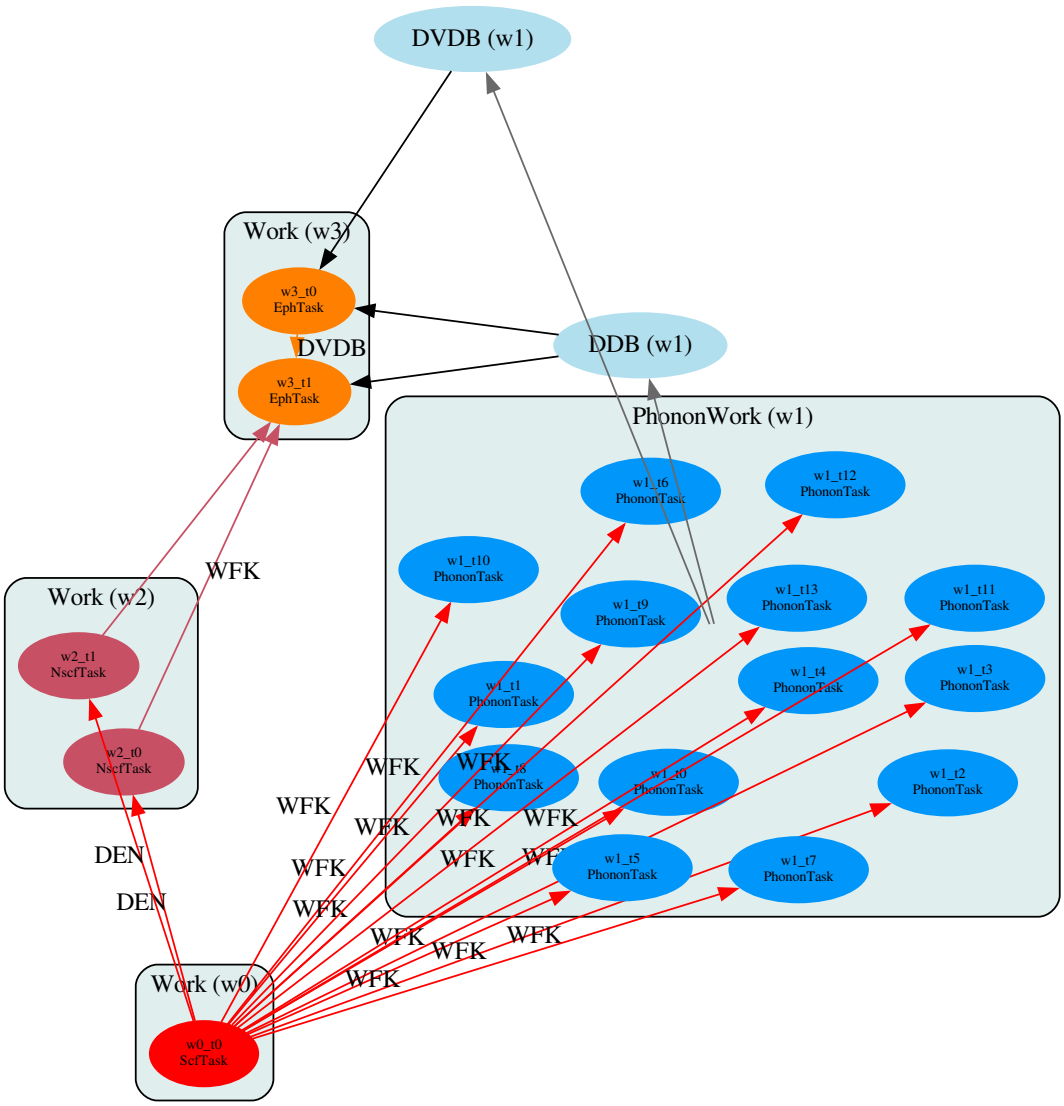

Figure 3.2: AbiPy workflow used for calculating transport properties in metallic systems.

```
LREAL    = .FALSE.
ADDGRID = .TRUE.
```

Phono3py then gathers the forces to calculate the third-order force-constants using the finite difference method, to finally compute the LTC using Eq. (2.22).

Chapter 4

Results

The calculated electrical resistivity/conductivity and thermal conductivity for Zr, ZrC, and ZrN are found in the following subsections. The electron band structures and phonon dispersions for each system are included in Appendix A. The relevant input parameters/dimensions for the EPH calculations are given in Table 4.1. It was found that the choice of RTA method (SERTA/MRTA) had little effect on the results. The primitive cell was used for all EPH calculations.

PAW potentials were used when computing the lattice thermal conductivity with Phono3py. The conventional cell was used with Phono3py instead of the primitive cell, and the results was calculated using both Abinit and Vasp for comparison. The relevant input parameters/dimensions for the Phono3py calculations with Vasp are given in Table 4.2.

	Zr	ZrC	ZrN
`ecut` (Ha)	50	50	50
coarse **k**/**q**-grid	12x12x12	16x16x16	14x14x14
interpolated **k**/**q**-grid	36x36x36	48x48x48	42x42x42
`sigma_erange`[1](eV)	±2.0	±2.0	±2.0
lattice constants (Å)	3.19, 5.11	4.67	4.55
space group	$P6_3/mmc$	$Fm\bar{3}m$	$Fm\bar{3}m$
RTA method	SERTA	MRTA	MRTA

Table 4.1: EPH calculations input parameters and relevant dimensions.

	Zr	ZrC	ZrN
cutoff energy (eV)	346	741	755
k-grid	6x6x6	4x4x4	6x6x6
q-grid	18x18x18	18x18x18	18x18x18
supercells	2x2x2	2x2x2	2x2x2
NN-distance (Å)	5.0	5.0	5.0
lattice constants (Å)	3.17, 5.09	4.70	4.58

Table 4.2: Phono3py with Vasp input parameters and relevant dimensions.

[1] `sigma_erange` selects the relevant k-points when evaluating the generalized transport coefficients. Since the derivative of the FD-distribution peaks at the Fermi-level, k-points away from this level contributes little to the integral and can be ignored to increase efficiency.

4.1 Zirconium

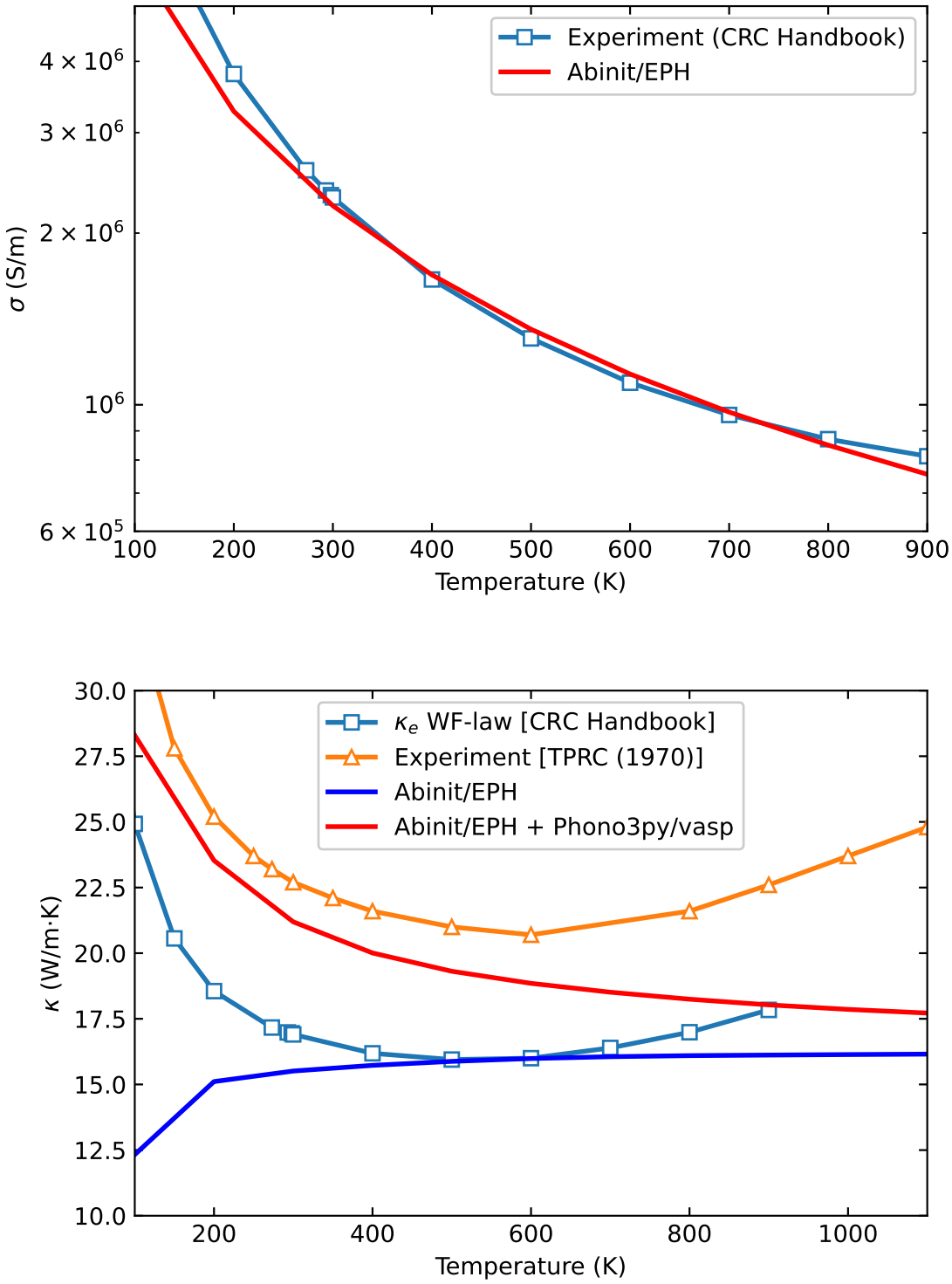

Figure 4.1: **Zr:** Electrical conductivity (top) and thermal conductivity (bottom).[9][34]

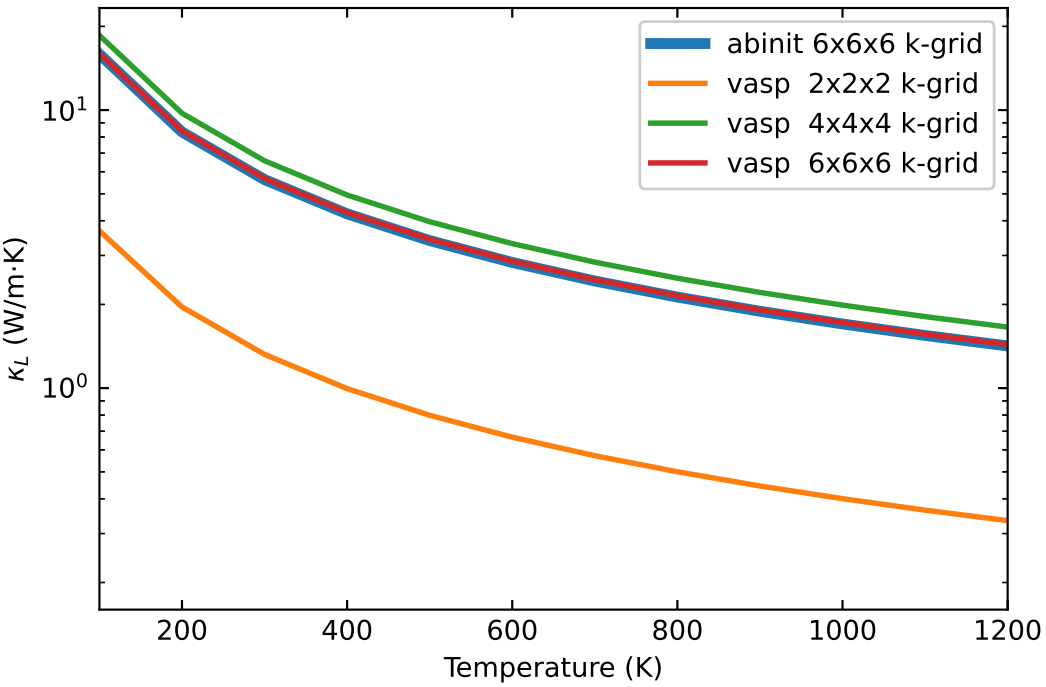

Figure 4.2: Convergence of the lattice thermal conductivity for Zr w.r.t the number of k-points.

Since Zirconium has an HCP structure up to 1136 K, the transport properties are anisotropic. The average values are shown in Fig. 4.1 and 4.2. Unfortunately the qualitative behavior in κ isn't quite captured by Abinit + phono3py above 600 K, with a maximum error of ∼40% at 1100 K. The cause of this is unknown as similar results were observed for sparser $\mathbf{k}/\mathbf{q}$-grids and smaller energy windows, so the results are believed to be sufficiently converged for $T > 300$ K. For $T < 300$ K, κ_e is not converged however since the derivative of the Fermi distribution is strongly peaked around the Fermi level for low temperatures, requiring a very dense sampling to reach convergence.

4.2 Zirconium carbide

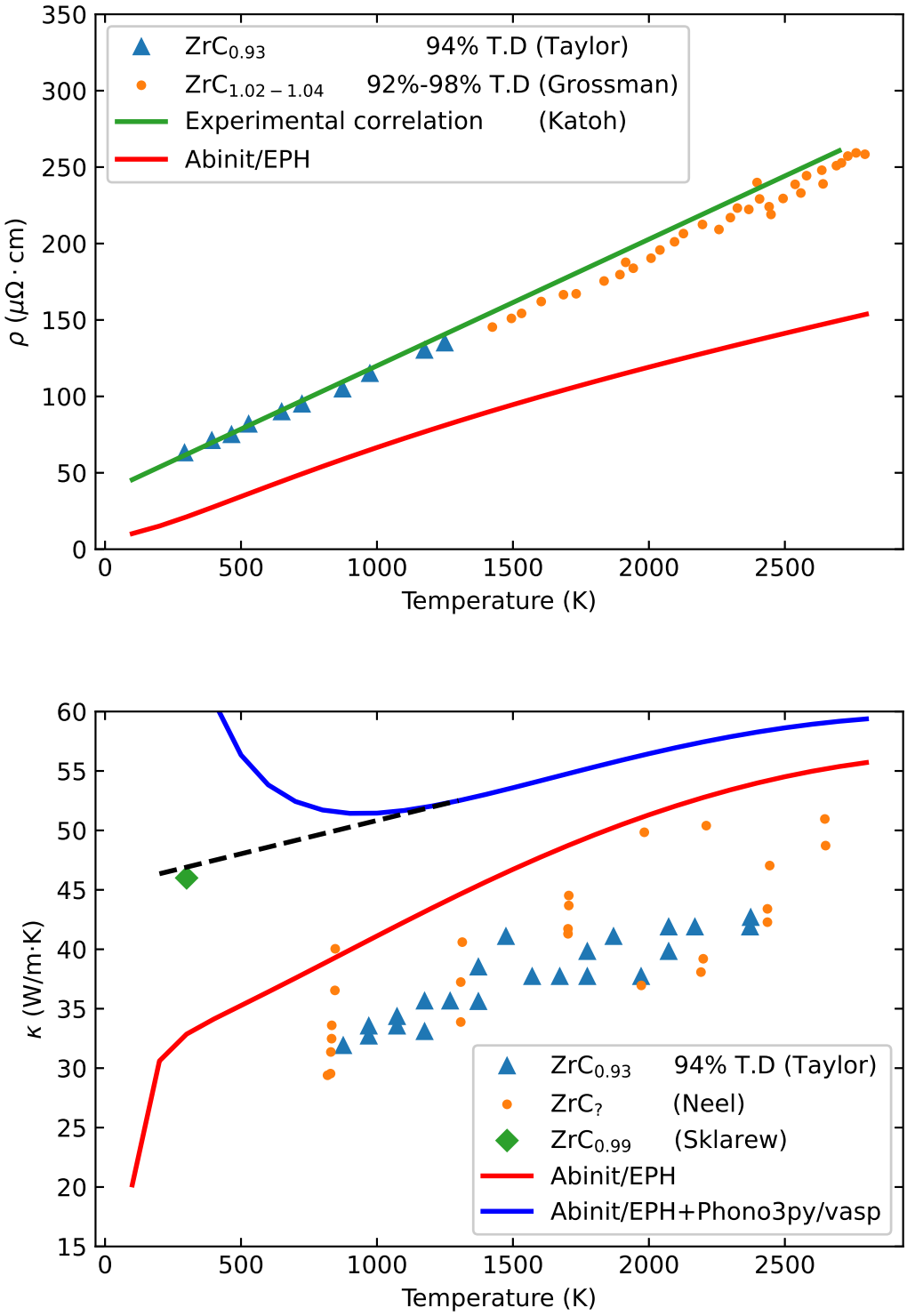

Figure 4.1: **ZrC:** Electrical resistivity (top) and thermal conductivity (bottom). The dashed line is the expected curve if electron-phonon interactions are taken into account for the LTC.[12][11][30][20][7][28]

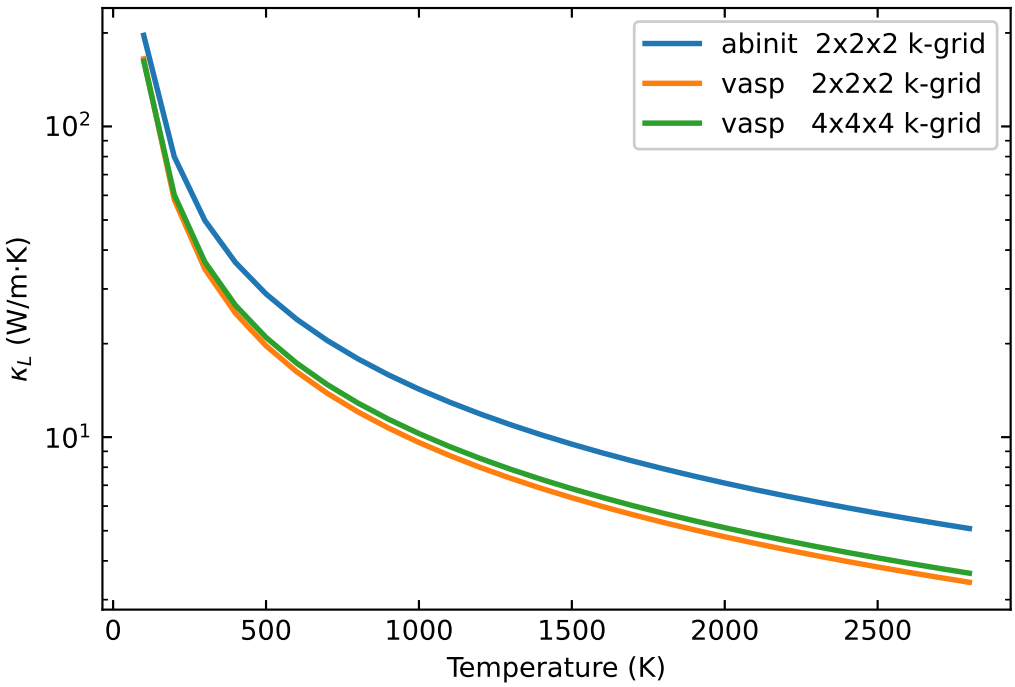

Figure 4.2: Convergence of the lattice thermal conductivity for ZrC w.r.t the number of k-points.

The electrical resistivity obtained from Abinit is significantly lower than the available reference data, which is suspected to be because of deviations from Zr/C = 1 in the data. Similarly, the thermal conductivity is higher than the experimental data. The one experimental data point at room temperature for ZrC that has near perfect stoichiometric ratio (Sklarew) is in line with the extrapolated thermal conductivity (dashed line in Fig. 4.1), which is the expected curve if electron-phonon interactions were included when computing the LTC. Ref. [11] and [12] shows that the thermal conductivity increases almost asymptotically near Zr/C = 1. This suggests that the calculated κ could be in agreement with the real thermal conductivity for a perfect crystal. The electrical conductivity exhibits similar asymptotic behavior near Zr/C = 1.[11][12]

4.3 Zirconium nitride

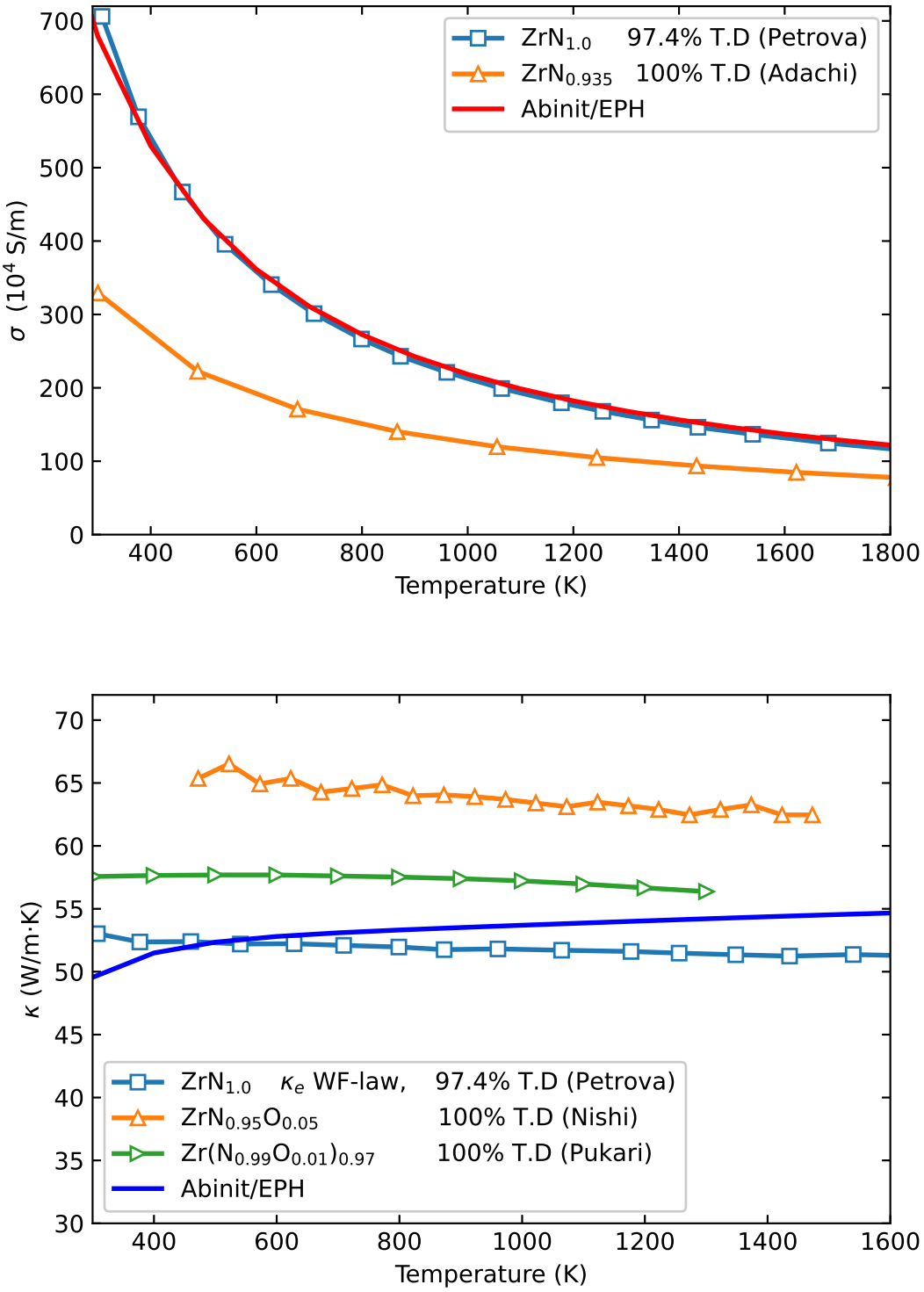

Figure 4.1: **ZrN:** Electrical conductivity (top) and thermal conductivity (bottom). No convergent lattice thermal conductivity could be obtained.[25][1][26][21]

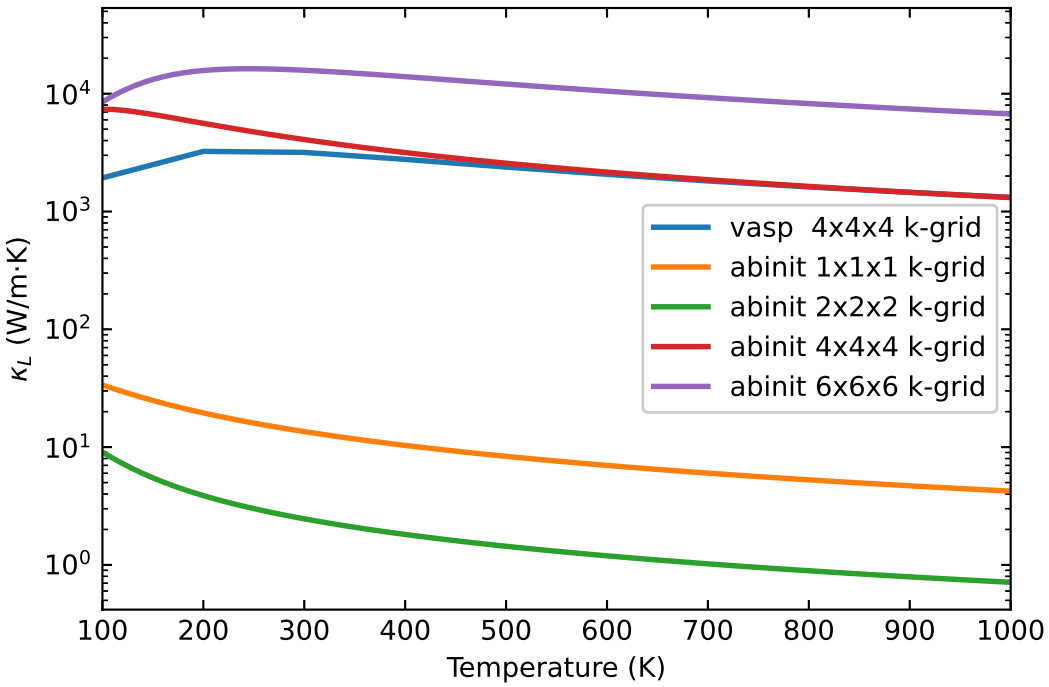

Figure 4.2: The lattice thermal conductivity for ZrN diverges w.r.t the number of k-points.

The electrical conductivity is in excellent agreement with experiment. As can be seen from the included experimental data, the stoiciometric ratio has an astounding effect on the resistivity and thermal conductivity, especially near a perfect crystal. Strangely, no convergent lattice thermal conductivity could be obtained from Phono3py as shown in Fig. 4.2, even though almost the same input parameters as for ZrC was used. The main source of error is the lack of electron-phonon interaction, and it could be that this scattering mode dominates for the entire temperature range. The LTC is usually on the order of 2-20 W/(m·K) for metals for intermediate/high temperatures, so the electronic contribution κ_e in Fig. 4.1 seems to be well within the real value.[33]

Notes

It was found that for higher temperatures, a greater energy span (`sigma_erange`) around the Fermi level is required but at the same time the grid size can also be reduced. This fact should be utilized in future works to speed up convergence by using different settings for different temperature ranges (i.e. low energy window and large grid-size for low temperatures).

Spin-polarized EPH calculations was attempted for ferromagnetic Nickel and Iron but showed poor agreement with experimental data. Spin-polarized calculations did however give the same result as non-polarized calculations for non-magnetic materials like Al and Cu.

Chapter 5

Conclusions

This project has demonstrated the capabilities of the Abinit EPH code to achieve a rather successful replication the electronic transport properties in non-magnetic Zr, ZrC, and ZrN. The calculated electrical resistivity for ZrC showed the greatest discrepancy with experiment and can hopefully provide a new reference value in other studies. The divergent lattice thermal conductivity of ZrN obtained from Phono3py should be further investigated.

The ultimate goal is to perform first principles transport calculations on irradiated uranium nitride, which is probably the most complicated system imaginable as it contains several dozen different elements (many of them actinides) and defects, placed in a disorderly fashion. Though great progress was made in this project, a number of obstacles need to be overcome before this can be achieved:

- Pseudo-potentials compatible with Abinit needs to be developed for the actinides,[1] something I hope the PseudoDojo project will provide in the future (work is currently being done on the lanthanides).
- Spin-polarized EPH calculations for magnetic systems should be resolved. Alternatively, since we are primarily interested in the high-temperature regime, investigate whether unpolarized calculations are sufficient above the Curie temperature.
- Since Uranium (indeed all actinides) exhibits strongly correlated electron behavior, DFT+U might be necessary to obtain correct results.[2]
- Support for PAW potentials in the EPH code. Though not strictly necessary, PAW potentials could increase performance significantly compared to norm-conserving potentials.

The primary challenge however is the modeling of defects and disordered lattices, which is known to have a defining impact on transport properties. A large enough simulation cell to accommodate the disorder (and to avoid self-interaction of atoms) will quickly

[1] Developing pseudo-potentials for the actinides and lanthanides are notoriously difficult as they are characterized by strong electron correlation effects.

[2] DFT+U is an extension of DFT that introduces a Hubbard-like term (U) into the DFT Hamiltonian. This Hubbard-like term accounts for the on-site Coulomb repulsion between localized electrons in a more accurate way, which helps to treat the strong electron correlations in systems with partially filled 5f and 6d orbitals like Uranium.

become computationally unfeasible; not only because of an increased number of atoms but also due to the breaking of symmetry. A natural next step would be to investigate the effect of each defect type separately in the dilute limit. That is, we assume that negligibly few defects are close enough to effect each other.

5.1 Future Work

The electron-phonon interaction from Eq. (2.25) and (2.26) should be included when computing the LTC to get a more complete model for metallic systems.

The next stepping stone would be to try to replicate the transport properties of a simple disordered alloy where experimental data is readily available, such as Cu_xAu_{1-x} in the dilute limit (i.e. x near 0 or 1).

Bibliography

[1] Adachi, Jun et al. "Thermal and electrical properties of zirconium nitride". In: *Journal of Alloys and Compounds* 399.1 (2005), pp. 242–244. ISSN: 0925-8388.

[2] Arovas, Daniel. *Lecture Notes on Condensed Matter Physics (A Work in Progress)*. Mar. 2010.

[3] Blundell, S.J. and Blundell, K.M. *Concepts in Thermal Physics*. OUP Oxford, 2010.

[4] Giustino, Feliciano. "Electron-phonon interactions from first principles". In: *Rev. Mod. Phys.* 89 (1 Feb. 2017).

[5] Gonze, Xavier et al. "The Abinit project: Impact, environment and recent developments". In: *Comput. Phys. Commun.* 248 (2020).

[6] Griffiths, David J. and Schroeter, Darrell F. *Introduction to Quantum Mechanics*. 3rd ed. Cambridge University Press, 2018.

[7] Grossman, Leonard N. "High-Temperature Thermophysical Properties of Zirconium Carbide". In: *Journal of the American Ceramic Society* 48.5 (1965), pp. 236–242.

[8] Hamann, D. R. "Optimized norm-conserving Vanderbilt pseudopotentials". In: *Phys. Rev. B* 88 (8 Aug. 2013), p. 085117.

[9] Haynes, W.M. *CRC Handbook of Chemistry and Physics*. CRC Handbook of Chemistry and Physics. CRC Press, 2014.

[10] Imbalzano, Giulio. *First principle calculations of the residual resistivity of defects in metals*. 2015.

[11] Jackson, H.F. and Lee, W.E. "2.13 - Properties and Characteristics of ZrC". In: *Comprehensive Nuclear Materials*. Ed. by Rudy J.M. Konings. Oxford: Elsevier, 2012, pp. 339–372. ISBN: 978-0-08-056033-5.

[12] Katoh, Yutai et al. "Properties of zirconium carbide for nuclear fuel applications". In: *Journal of Nuclear Materials* 441.1 (2013), pp. 718–742. ISSN: 0022-3115.

[13] Kittel, C. and McEuen, P. *Introduction to Solid State Physics*. John Wiley & Sons, Limited, 2018.

[14] Kresse, G. and Furthmüller, J. "Efficiency of ab-initio total energy calculations for metals and semiconductors using a plane-wave basis set". In: *Computational Materials Science* 6.1 (1996), pp. 15–50. ISSN: 0927-0256.

[15] Kresse, G. and Furthmüller, J. "Efficient iterative schemes for ab initio total-energy calculations using a plane-wave basis set". In: *Phys. Rev. B* 54 (16 Oct. 1996), pp. 11169–11186.

[16] Kresse, G. and Joubert, D. “From ultrasoft pseudopotentials to the projector augmented-wave method”. In: *Phys. Rev. B* 59 (3 Jan. 1999), pp. 1758–1775.

[17] Li, Shouhang et al. “Thermal conductivity and Lorenz ratio of metals at intermediate temperatures with mode-level first-principles analysis”. In: *Phys. Rev. B* 102 (17 Nov. 2020).

[18] Marques, Miguel A.L., Oliveira, Micael J.T., and Burnus, Tobias. “Libxc: A library of exchange and correlation functionals for density functional theory”. In: *Comput. Phys. Commun.* 183.10 (Oct. 2012), pp. 2272–2281.

[19] Martin, Richard M. *Electronic Structure: Basic Theory and Practical Methods*. 2nd ed. Cambridge University Press, 2020.

[20] Neel, D.S., Pears, C.D., and Oglesby, S. *The Thermal Properties of Thirteen Solid Materials to 5000 °F for their Destruction Temperatures*. Southern Research Institute: Birmingham, A, 1962.

[21] Nishi, Tsuyoshi et al. “Thermal Conductivities of Zr-based Transuranium Nitride Solid Solutions”. In: *Journal of Nuclear Science and Technology* 48.3 (2011), pp. 359–365.

[22] Peng, Jie et al. “Thermal conductivity of -U with point defects”. In: *Journal of Applied Physics* 130.18 (Nov. 2021). ISSN: 0021-8979.

[23] Perdew, John P., Burke, Kieron, and Ernzerhof, Matthias. “Generalized Gradient Approximation Made Simple”. In: *Phys. Rev. Lett.* 77 (18 Oct. 1996), pp. 3865–3868.

[24] Perdew, John P. et al. “Restoring the Density-Gradient Expansion for Exchange in Solids and Surfaces”. In: *Physical Review Letters* 100.13 (Apr. 2008).

[25] Petrova, I.I. et al. “Investigation of the electrical resistivity of zirconium and hafnium nitrides”. In: *TVT* 10 (5 1972), pp. 1007–1012. URL: `http://mi.mathnet.ru/tvt10633`.

[26] Pukari, Merja, Takano, Masahide, and Nishi, Tsuyoshi. “Sintering and characterization of (Pu,Zr)N”. In: *Journal of Nuclear Materials* 444.1 (2014), pp. 421–427. ISSN: 0022-3115.

[27] Singh, J. *Modern Physics for Engineers*. Wiley, 2008.

[28] Sklarew, S and Albom, MJ. “Pyrolytically Derived Refractory Materials for Aerospace Applications”. In: *The Marquardt Corp., Van Nuys, CA* (1963).

[29] Srivastava, G.P. *The Physics of Phonons*. Taylor & Francis, 1990.

[30] Taylor, R.E. “Thermal Conductivity of Zirconium Carbide at High Temperatures”. In: *Journal of the American Ceramic Society* 45.7 (1962), pp. 353–354.

[31] Thijssen, Jos. *Computational Physics*. 2nd ed. Cambridge University Press, 2007.

[32] Togo, Atsushi, Chaput, Laurent, and Tanaka, Isao. “Distributions of phonon lifetimes in Brillouin zones”. In: *Physical Review B* 91.9 (2015).

[33] Tong, Zhen et al. “Comprehensive first-principles analysis of phonon thermal conductivity and electron-phonon coupling in different metals”. In: *Phys. Rev. B* 100 (14 Oct. 2019), p. 144306.

[34] Touloukian, Y.S. et al. *Thermophysical Properties of Matter - The TPRC Data Series. Volume 1. Thermal Conductivity - Metallic Elements and Alloys*. Defense Technical Information Center, 1970.

[35] van Setten, M.J. et al. "The PseudoDojo: Training and grading a 85 element optimized norm-conserving pseudopotential table". In: *Computer Physics Communications* 226 (2018), pp. 39–54. ISSN: 0010-4655.

[36] Xu, Bin and Verstraete, Matthieu J. "First Principles Explanation of the Positive Seebeck Coefficient of Lithium". In: *Physical Review Letters* 112.19 (2014).

[37] Ziman, J.M. *Electrons and Phonons: The Theory of Transport Phenomena in Solids*. Oxford University Press, Feb. 2001.

Appendix A

Electron band structure and phonon dispersion

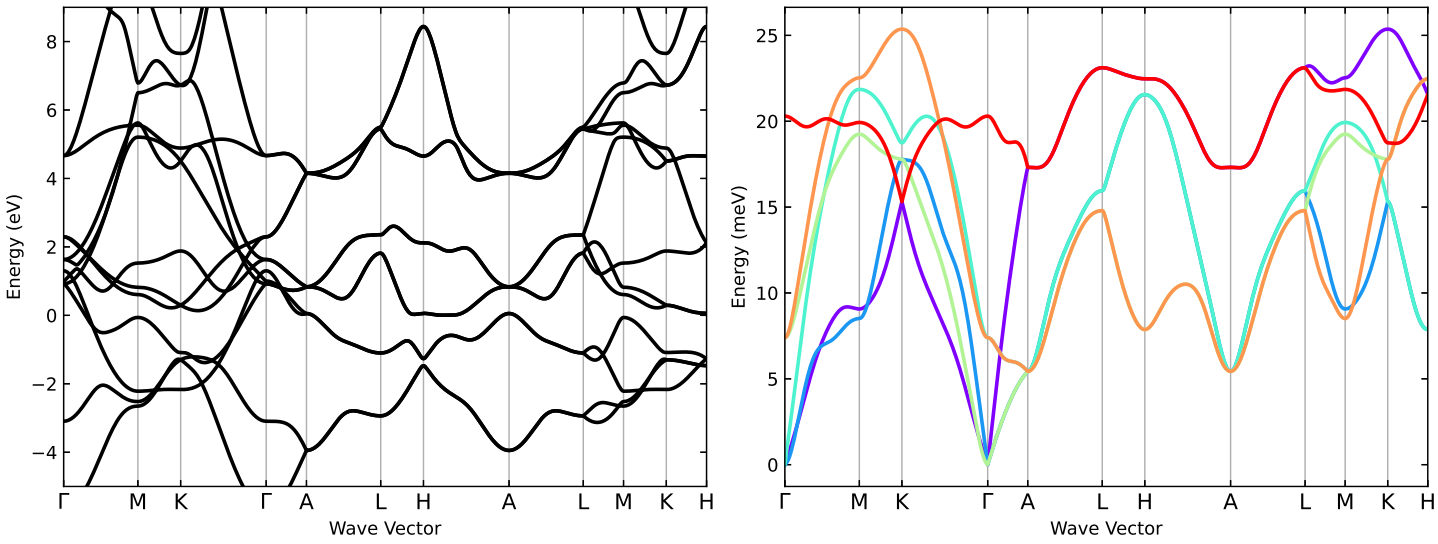

Figure A.1: **Zr**

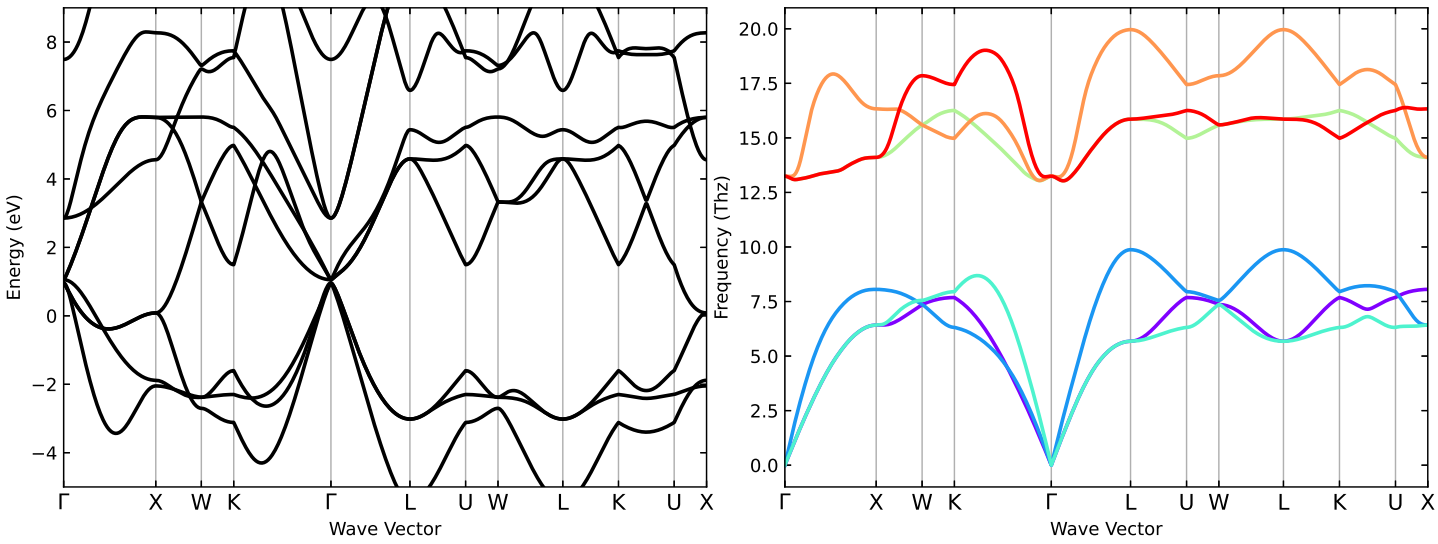

Figure A.2: **ZrC**

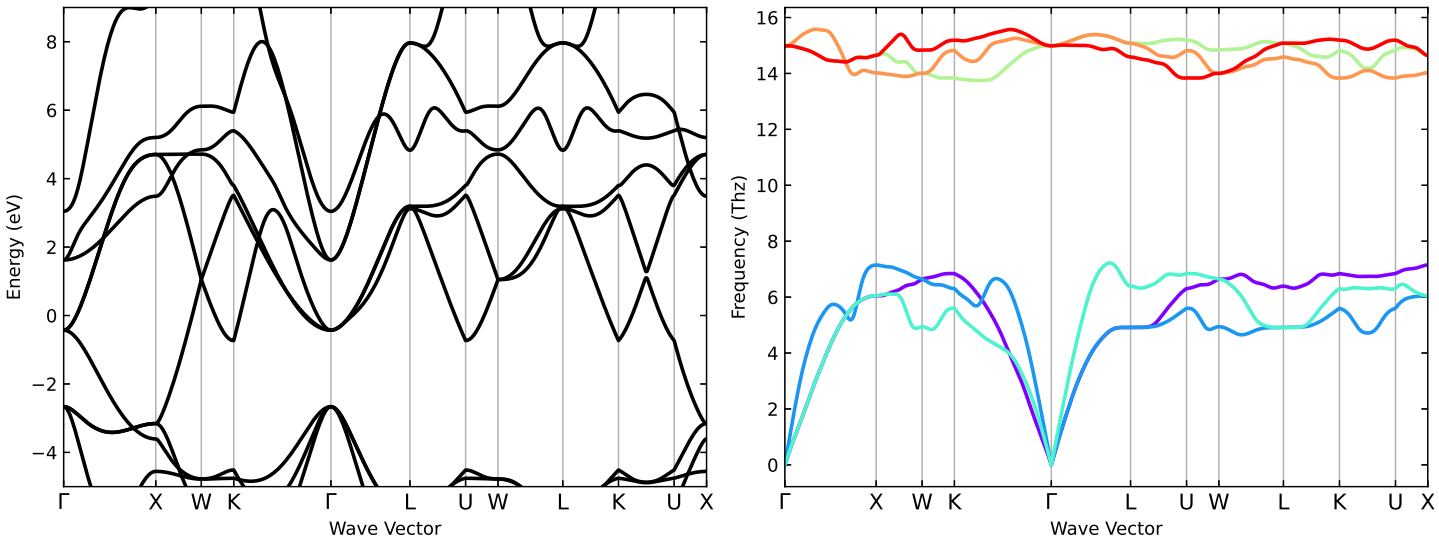

Figure A.3: **ZrN**